

MIP1, a New Yeast Gene Homologous to the Rat Mitochondrial Intermediate Peptidase Gene, Is Required for Oxidative Metabolism in *Saccharomyces cerevisiae*

GRAZIA ISAYA,* DAVID MIKLOS, AND ROBERT A. ROLLINS

Department of Genetics, Yale University School of Medicine, New Haven, Connecticut 06520-8005

Received 18 April 1994/Returned for modification 18 May 1994/Accepted 25 May 1994

Cleavage of amino-terminal octapeptides, F/L/IXXS/T/GXXXX, by mitochondrial intermediate peptidase (MIP) is typical of many mitochondrial precursor proteins imported to the matrix and the inner membrane. We previously described the molecular characterization of rat liver MIP (RMIP) and indicated a putative homolog in the sequence predicted from gene *YCL57w* of yeast chromosome III. A new yeast gene, *MIP1*, has now been isolated by screening a *Saccharomyces cerevisiae* genomic library with an RMIP cDNA probe. *MIP1* predicts a protein of 772 amino acids (YMIP), which is 54% similar and 31% identical to RMIP and includes a putative 37-residue mitochondrial leader peptide. RMIP and YMIP contain the sequence LFHEMGGHAM HSMLGRT, which includes a zinc-binding motif, HEXXH, while the predicted *YCL57w* protein contains a comparable sequence with a lower degree of homology. No obvious biochemical phenotype was observed in a chromosomally disrupted *ycl57w* mutant. In contrast, a *mip1* mutant was unable to grow on nonfermentable substrates, while a *mip1 ycl57w* double disruption did not result in a more severe phenotype. The *mip1* mutant exhibited defects of complexes III and IV of the respiratory chain, caused by failure to carry out the second MIP-catalyzed cleavage of the nuclear-encoded precursors for cytochrome oxidase subunit IV (CoxIV) and the iron-sulfur protein (Fe-S) of the *bc₁* complex to mature proteins. In vivo, intermediate-size CoxIV was accumulated in the mitochondrial matrix, while intermediate-size Fe-S was targeted to the inner membrane. Moreover, *mip1* mitochondrial fractions failed to carry out maturation of the human ornithine transcarbamylase intermediate (iOTC), specifically cleaved by RMIP. A *CEN* plasmid-encoded YMIP protein restored normal MIP activity along with respiratory competence. Thus, YMIP is a functional homolog of RMIP and represents a new component of the yeast mitochondrial import machinery.

Mitochondrial intermediate peptidase (MIP; EC 3.4.24.93D) is a thiol-dependent metallopeptidase localized to the mitochondrial matrix and involved in two-step processing of a heterogeneous subgroup of imported mitochondrial precursor proteins (24, 27). These precursors, targeted to the matrix or the inner membrane, are initially cleaved by a general mitochondrial processing peptidase (MPP; EC 3.4.99.41) (19, 31, 35, 57) which removes most of the targeting signal, leaving a characteristic octapeptide sequence (F/L/I/XXS/T/GXXXX) (14, 20) at the protein amino terminus. The resulting intermediate-size proteins are then processed to mature subunits by MIP, which specifically cleaves off the octapeptides (25).

MIP has been purified to homogeneity from rat liver mitochondrial matrix (28), and a full-length cDNA has been isolated (26). Sequence analysis revealed that rat MIP (RMIP) is structurally related to a putative metallopeptidase predicted from the sequence of gene *YCL57w* of yeast chromosome III (34). Because a typical mitochondrial targeting signal was found at the amino terminus of this protein sequence, we proposed that *YCL57w* might encode a yeast homolog of RMIP (26).

Previous studies of *Saccharomyces cerevisiae* (6, 12, 15, 22) and *Neurospora crassa* (17, 51) suggest that the MIP-dependent pathway of mitochondrial enzyme maturation is conserved in lower eukaryotes. MIP has not been characterized in these microorganisms, however, and its role in mitochondrial

biogenesis and cell viability is not known (1). In *S. cerevisiae*, at least two mitochondrial protein precursors are processed to mature subunits in two steps via formation of an octapeptide-containing intermediate, the Rieske iron-sulfur protein (Fe-S) of the *bc₁* complex (6, 12, 15), and cytochrome oxidase subunit IV (CoxIV) (22). We reasoned that, if MIP activity is relevant to Fe-S and CoxIV biogenesis and, ultimately, respiratory chain function, inactivation of a putative yeast MIP gene should cause accumulation of uncleaved intermediate proteins and, thereby, render the cell deficient in oxidative metabolism. By this approach, we show here that *YCL57w* is not responsible for MIP activity in *S. cerevisiae*. Rather, a newly isolated sequence more closely related to RMIP, *MIP1*, encodes a functional homolog of mammalian MIP and is required for mitochondrial respiratory competence.

MATERIALS AND METHODS

Yeast strains, growth media, and plasmids. The following previously described strains were used: YPH501 (*MATa/MAT α ura3-52/ura3-52 lys2-801^{amber}/lys2-801^{amber} ade2-101^{ochre}/ade2-101^{ochre} trp1- Δ 63/trp1- Δ 63 his3- Δ 200/his3- Δ 200 leu2- Δ 1/leu2- Δ 1) (46), AW1-2 (*MATa/MAT α ura3-52/ura3-52 leu2-3,112/leu2-3,112*) (54), α 429c (*MAT α mif1-1 his4-519 ura3-52 leu2-3,112 arg3*) (35), and B35.1 (*MAT α mif2-1 his4-519 ura3-52 leu2-3,112 arg3*) (54). The following mutants were constructed in this study: *mip1* disruption strains Y6040, a YPH501 derivative (*MAT α ura3-52 lys2-801^{amber} ade2-101^{ochre} trp1- Δ 63 his3- Δ 200 leu2- Δ 1 mip1 Δ ::LEU2*), and Y34, an AW1-2 derivative (*MAT α ura3-52 leu2-3,112 mip1 Δ ::LEU2*); *ycl57w* disruption strain Y191, an AW1-2 derivative (*MATa ura3-52 leu2-3,112**

* Corresponding author. Mailing address: Department of Genetics, Yale University School of Medicine, 333 Cedar Street, P.O. Box 208005, New Haven, CT 06520-8005. Phone: (203) 785-4840. Fax: (203) 785-7227.

ycl57wΔ::LEU2); and *mip1 ycl57w* double-disruption strain DKO1, a Y34 derivative (*MATα ura3-52 leu2-3,112 mip1Δ::LEU2 ycl57wΔ::URA3*).

The following liquid and solid media were used: YPD (2% glucose, 2% peptone, 1% yeast extract), YPGal (2% galactose, 2% peptone, 1% yeast extract), YPEG (3% glycerol, 2% ethanol, 2% peptone, 1% yeast extract), SD (2% dextrose, 6.7% Bacto-yeast nitrogen base without amino acids) (Difco), and semisynthetic medium (3% glycerol, 2% ethanol, 0.05% dextrose, 6.7% Bacto-yeast nitrogen base without amino acids, 0.3% yeast extract). Unless otherwise stated, all amino acids and other growth requirements of the parental AW1-2 or YPH501 were added to liquid and solid SD medium at the normally recommended concentrations (45).

Plasmids pBluescript (Stratagene) and pGEM-3Z (Promega) were used for subcloning, sequencing, and DNA manipulations. The *LEU2* gene was excised from plasmid YEp13 (5), and the *URA3* gene was excised from plasmid YEp24 (3). A centromere plasmid, YCp50 (37), carrying the *URA3* gene, was used for complementation studies. Plasmid pGALOTC has been described before (7). This construct consists of the cDNA encoding the human ornithine transcarbamylase precursor (pOTC) joined to plasmid pCGS109, which contains a 2- μ m replication origin, the *URA3* gene, and the inducible *GALI1* promoter.

Cloning of *MIP1* by library screening. A λ DASH yeast genomic library (Stratagene) was screened by use of a random primer-labeled (Boehringer Mannheim) full-length RMIP cDNA probe (26). Hybridization of Hybond-N nylon membrane filters (Amersham Corp.) was carried out in 6 \times SSC (1 \times SSC is 0.15 M NaCl plus 0.015 M sodium citrate, pH 7.0)–5 \times Denhardt's solution (1 \times Denhardt's solution is 0.02% polyvinylpyrrolidone–0.02% Ficoll–0.02% bovine serum albumin [BSA])–10% dextran sulfate–1% sodium dodecyl sulfate (SDS), containing 100 μ g of salmon sperm DNA per ml, for over 18 h at 62°C. Filters were washed twice for 10 min in 2 \times SSC–0.5% SDS at room temperature and twice for 20 min in 1 \times SSC–0.5% SDS at 58°C. Autoradiograms were developed after each washing step. Phage λ DNA was prepared from positive plaques isolated after tertiary screening by standard procedures (40) and subjected to Southern blotting under the hybridization conditions described above, except that washings were carried out at higher stringency in 0.1 \times SSC–0.5% SDS at 65°C. Specific DNA fragments were cloned in pBluescript and analyzed by sequencing from both strands with Sequenase (U.S. Biochemicals) with universal and specific primers and subcloned restriction fragments. The following degenerate primer, based on the putative RMIP zinc-binding site sequence, was used for initial identification of the *MIP1* gene: 5'-GAA/GATGGGNCAT/CGCNATGCA-3' (see Fig. 1).

Cloning of *YCL57w* by PCR amplification. For cloning of *YCL57w*, 2 μ g of total genomic yeast DNA isolated from strain AW1-2 was PCR amplified by use of the following primers on the basis of the published sequence of yeast chromosome III (34): sense primer, 5'-AACCCGGGCGAAGTAATAGCTGCTGATTGGTCAGAAT-3' (nucleotides 24444 to 24473 of the chromosome III sequence, including an *SmaI* site at the 5' end); antisense primer, 5'-TTAAGCTTCCTAGGCGTGGTCAACGATAAGTTATATGT-3' (nucleotides 27210 to 27239, including an *HindIII* site at the 5' end). PCRs (100 μ l) were carried out in the presence of 100 nM (each) primer and 200 μ M (each of the four) dinucleoside triphosphates in a buffer containing 10 mM Tris-HCl (pH 8.3), 50 mM KCl, 1.5 mM MgCl₂, 4 U of *Taq* polymerase (Cetus), and 10% dimethyl sulfoxide for 30 cycles of 1.5 min at 94°C, 1.5 min at 65°C, and 1.5 min at 72°C. A PCR-amplified 2.8-kbp fragment, predicted

to contain the *YCL57w* coding sequence plus 0.3 kbp of 5' sequence and 0.4 kbp of 3' sequence, was isolated, digested with *SmaI* and *HindIII*, cloned into an *SmaI-HindIII*-digested pGEM-3Z plasmid, and analyzed by DNA sequencing, as described above. PCR amplifications of the *YCL57w* sequence were also carried out directly on positive plaques isolated from primary screening of a λ DASH yeast genomic library. Plaques were picked from agar plates, placed in 1 ml of SM buffer (100 mM NaCl–10 mM MgSO₄–50 mM Tris-HCl [pH 7.5]–2% gelatin), and left at room temperature for 3 h to allow λ DNA to diffuse out of the agar. SM buffer (20 μ l from each plaque) was used in PCRs under the conditions described above with specific primers designed such that the 3' half of *YCL57w* would be amplified: 5'-CAGATCCAACTACTACATTTGGGACCAC-3' (sense primer; nucleotides 25800 to 25829 of *YCL57w*) and 5'-AACGAATTTAGTTCTGTAAGCCCAGCTCC-3' (antisense primer; nucleotides 26897 to 26869 of *YCL57w*). Amplified fragments were analyzed by sequencing, as described above.

Chromosomal disruptions. For construction of the deletion allele *mip1Δ::LEU2*, a 4.6-kbp *AccI-AccI* fragment, containing *MIP1* plus 0.9 kbp of 5' flanking sequences and 1.4 kbp of 3' flanking sequences (see Fig. 1), was filled in and cloned into the *EcoRV* site of pBluescript. By digestion with *SmaI* and *HindIII*, the entire fragment was excised from the pBluescript polylinker and subcloned into pGEM-3Z. This construct was digested with *NaeI* and *EcoNI*, removing the internal 2,053 nucleotides coding for residues 31 to 717 of *YMIP*. They were replaced with a 2.2-kbp *SalI-XhoI* fragment from the YEp13 plasmid carrying the yeast *LEU2* gene (5) (see Fig. 4). A linear *AvaI-HindIII* fragment, containing the *mip1Δ::LEU2* allele plus the 5' and 3' flanking sequences, was used for integrative DNA transformation (39) of diploid strains AW1-2 and YPH501. Following sporulation and tetrad dissection, haploid cells containing the *mip1Δ::LEU2* allele were identified on the basis of ability to grow on SD from which only leucine was missing [SD(–Leu)] and by Southern blotting.

For construction of the *ycl57wΔ::LEU2* allele, a pGEM-3Z plasmid containing the PCR-amplified *YCL57w* coding sequence plus 5' and 3' untranslated sequences was digested with *ApaI* and *BamHI*, removing the internal 1,717 nucleotides coding for residues 92 to 663 of the *YCL57w* protein sequence. These were replaced with the yeast *LEU2* gene. A linear *SmaI-HindIII* fragment was used for integrative DNA transformation of diploid strain AW1-2. After sporulation and dissection, haploid cells carrying the *ycl57wΔ::LEU2* allele were identified by ability to grow on SD(–Leu) and Southern blotting.

For construction of the *ycl57wΔ::URA3* allele, the internal 1,717 nucleotides coding for residues 92 to 663 of the *YCL57w* protein sequence were replaced with a 1.1-kbp *HindIII-SmaI* fragment from the YEp24 plasmid carrying the yeast *URA3* gene, as described above. A linear *SmaI-HindIII* fragment was used for integrative DNA transformation of *mip1* disruption mutant Y34, and transformants carrying both the *mip1Δ::LEU2* and *ycl57wΔ::URA3* alleles were identified by ability to grow on SD(–Leu –Ura). The double chromosomal disruption was confirmed by PCR and Southern blotting.

Standard procedures were used for lithium acetate transformation of yeast cells, sporulation and tetrad dissection, total genomic yeast DNA isolation (38), and Southern blotting (40).

Construction of a *MIP1* fusion gene with a c-myc epitope. To construct a *MIP1* gene coding for a chimeric protein with a carboxyl-terminal c-myc (9E10) epitope (11), the 3' end of the gene was modified by introducing the epitope-encoding nucleotide sequence at the sequence corresponding to codon 772

and stop codon 773. Two overlapping DNA products were initially synthesized via PCR. A 279-bp PCR product was synthesized with the following primers: 5'-CGATCAGAGTAATTGGTGTGGAAGATTCGG-3' (sense primer 1), overlapping the sequence from nucleotide 2160 to nucleotide 2190 upstream from a unique *Eco*NI site at position 2269 of the *MIP1* coding sequence, and 5'-AGACTTGTGAGACTGTGCTATAAATTCAT-3' (antisense primer 2), overlapping the sequence from nucleotide 2439, near the *MIP1* stop codon, to nucleotide 2409. A second 466-bp PCR product was amplified with the following primers: 5'-ATGGAATTTATAGCAGTCTCACAAGTCTGAACAGAACTTATTTCTGAAGAAGACTTGTAGAGAACAGAGTAGGTGCTTAA-3' (sense primer 3), overlapping the *MIP1* sequence from nucleotide 2409 to nucleotide 2462 and containing the *c-myc* coding sequence, and 5'-TTAAGCTTAAGCTGCAGGAAGTGAGTTCGTA-3' (antisense primer 4), overlapping the sequence from nucleotide 2971 to nucleotide 2944 of the *MIP1* 3' untranslated region (not shown in Fig. 2) and including a *Hind*III site at the 5' end. An 811-bp PCR product, from nucleotide 2160 to nucleotide 2971, was subsequently synthesized in a reaction mixture containing 10 ng each of the 279- and 466-bp PCR products plus 200 μ M (each) sense primer 1 and antisense primer 4. After digestion with *Eco*NI and *Hind*III, this PCR product was substituted for a 1.5-kbp *Eco*NI-*Hind*III fragment in the original 4.6-kbp insert, containing *MIP1* and its 5' and 3' flanking sequences, in pGEM-3Z. DNA sequencing showed that ligation had yielded an in-frame fusion of the *MIP1* and *c-myc* epitope reading frames.

Complementation by *MIP1* or *MIP1-c-myc* on a centromere plasmid. For construction of a *mip1* Δ ::*LEU2* mutant complemented by a plasmid copy of wild-type *MIP1*, a 4.6-kbp *AccI*-*AccI* fragment, containing *MIP1* plus 0.9 kbp of 5' and 1.4 kbp of 3' flanking sequences, was excised from pBluescript by digestion with *Bam*HI and *Hind*III and subcloned into a *Bam*HI-*Hind*III-digested centromere plasmid, YCp50, carrying the yeast *URA3* gene (37). Similarly, a 3.4-kbp *Ava*I-*Hind*III fragment, containing the *MIP1-c-myc* fusion gene plus 650 bp of 5' and 440 bp of 3' flanking sequences, was excised from pGEM-3Z and subcloned into YCp50, as described above. These constructs were introduced via transformation into a heterozygous *mip1* disruption strain. Following sporulation and tetrad dissection, haploid cells containing the *mip1* Δ ::*LEU2* allele and the [*CEN-MIP1*] or [*CEN-MIP1-c-myc*] plasmid were identified on the basis of their ability to grow on SD(-Leu -Ura).

Analysis of total cell extracts. Yeast total cell extracts were prepared from 1-ml cell culture aliquots at an optical density at 600 nm (OD_{600}) of 1. Total proteins were precipitated with 10% trichloroacetic acid for 20 min on ice and then centrifuged in a microcentrifuge for 20 min at 4°C; the pellet was washed twice with acetone, dried, subjected to glass bead lysis by vortexing for 1 min in boiling buffer (10 mM Tris-HCl [pH 8.0]-25 mM EDTA-1% SDS), and immediately placed in a boiling water bath for 5 min. For immune blotting analysis, aliquots from these extracts were loaded directly on 9% T-4% C (for Fe-S detection) or 13% T-4% C (for CoxIV detection) SDS-polyacrylamide gels (T denotes the total concentration of acrylamide and bis-acrylamide; C denotes the percentage concentration of the cross-linker relative to T) and blotted to nitrocellulose membranes (Gelman Sciences). Protein detection was by an enhanced chemiluminescence procedure with reagents from Amersham. For Fe-S detection, we used a mouse anti-yeast Fe-S monoclonal antibody (a gift of B. Trumpower, Department of Biochemistry, Dartmouth Medical School) (15) followed by a horseradish peroxidase-conjugated

goat anti-mouse immunoglobulin G antiserum (Bio-Rad). For CoxIV detection, a rabbit anti-yeast CoxIV serum (a gift of G. Schatz, Biozentrum, Basel University) (21) was used, followed by a horseradish peroxidase-conjugated donkey anti-rabbit immunoglobulin G antiserum (Amersham). For cytochrome *c*₁ immune blotting, we used a mouse anti-yeast cytochrome *c*₁ monoclonal antibody (a gift of B. Trumpower).

For in vivo labeling, cells were grown in SD medium containing the appropriate growth requirements to an OD_{600} of 1 and labeled with 0.1 mCi of Tran³⁵S-Label (ICN Biochemicals) per ml for 24 min at 30°C. Labeling was stopped by addition of 0.5% unlabeled methionine and 0.5% unlabeled cysteine, and the cells were chased at 30°C for 60 min. Aliquots (1 ml) were withdrawn at the indicated time points, and total cell extracts were prepared from each aliquot as described above. Immunoprecipitation was performed on these extracts in NETMS buffer (150 mM NaCl-10 mM EDTA-0.5% Triton X-100-0.25% SDS-2% methionine) as described elsewhere (23). A rabbit anti-yeast CoxIV serum was used for detection of CoxIV protein (21), while a rabbit anti-rat OTC serum was used for detection of pGALOTC-encoded OTC protein, as described elsewhere (7). Immune complexes were recovered with formalin-fixed Staph A cells (Bethesda Research Laboratories), and radiolabeled proteins were analyzed by SDS-polyacrylamide gel electrophoresis (SDS-PAGE) and fluorography, as described before (23).

Analysis of isolated yeast mitochondria and mitochondrial subfractions. For isolation of mitochondria, *mip1* and wild-type cells were grown in YPGal containing 0.05% dextrose, while disruption strains complemented by a [*CEN-MIP1-c-myc*] plasmid were grown in semisynthetic medium containing 3% glycerol, 2% ethanol, and 0.05% dextrose. All strains were grown at 30°C to an OD_{600} of 1. Spheroplasts were prepared by treatment with Zymolyase 20T (ICN Immunobiologicals) and resuspended in mitochondria isolation buffer (MIB), containing 0.6 M mannitol and 20 mM HEPES (*N*-2-hydroxyethylpiperazine-*N'*-2-ethanesulfonic acid)-KOH, pH 7.4. Mitochondria were subsequently isolated by homogenization with a motor-driven Teflon pestle in a glass tissue grinder at a speed of 1,000 rpm, followed by differential centrifugation, according to the procedure described by Daum et al. (8). Phenylmethylsulfonyl fluoride was added at a final concentration of 10 mM during homogenization and was omitted from the subsequent washing steps. Freshly isolated mitochondria were resuspended in MIB and adjusted to a protein concentration of 20 mg/ml. Aliquots (25 or 50 μ l) were treated with trypsin (final concentration, 0.4 mg/ml) for 5 min on ice, and soybean trypsin inhibitor (final concentration, 1 mg/ml) was added; 1% Triton X-100 was added to other aliquots before trypsin. To prepare mitoplasts by osmotic shock, mitochondria were diluted with 5 volumes of 20 mM HEPES-KOH (pH 7.4) for 10 min on ice with occasional agitation on a Vortex mixer, as described elsewhere (56). Mitoplasts were reisolated by centrifugation at 12,000 \times g for 5 min, resuspended in the original volume of MIB buffer, and treated with trypsin, as described above.

To prepare soluble (matrix plus intermembrane space) and membrane (outer and inner membrane) mitochondrial fractions, mitochondria were resuspended in MIB (500 μ l at 20 mg/ml for mitochondria isolated from *mip1* and wild-type cells and 1 ml at 50 mg/ml for mitochondria isolated from [*CEN-MIP1-c-myc*]-complemented cells) and subjected to sonication at 0 to 4°C (with a Branson sonifier with microtip; setting on 20% duty, three 45-s pulses with two 1-min cooling intervals), followed by centrifugation at 165,000 \times g for 30 min at 4°C. Pellets were resuspended by pipetting in MIB buffer and brought to the same volume as supernatants. Protein concen-

tration was measured in all fractions by a protein assay from Bio-Rad based on the Bradford dye-binding procedure (4). Fractions were aliquoted and kept at -70°C for subsequent analyses.

Detection of Fe-S and CoxIV proteins in intact mitochondria and mitochondrial soluble and membrane fractions was by immune blotting, as described above. Detection of the YMIP-*c-myc* fusion protein was also by immune blotting, with a *c-myc* (9E10) mouse monoclonal antibody (11) (Santa Cruz Biotechnology, Inc.), followed by a horseradish peroxidase-conjugated goat anti-mouse immunoglobulin G antiserum (Bio-Rad). Protein quantitations were by densitometric analysis of fluorograms.

Import of YMIP and YMIP-*c-myc* into isolated rat liver and yeast mitochondria. The *MIP1* and *MIP1-c-myc* genes, cloned in pGEM-3Z under phage T7 polymerase promoter control, were transcribed in vitro, and mRNAs were translated in a reticulocyte lysate in the presence of [^{35}S]methionine, by use of a coupled transcription/translation system from Promega. Translation products were analyzed by SDS-PAGE with in vitro-translated RMIP precursor (78 kDa) (26) as a molecular mass marker.

For isolation of rat liver mitochondria, we used a modification of the procedure originally described by Schnaitman and Greenawalt (41), as described before (24). Briefly, liver tissue from one male Sprague-Dawley rat, weighing 90 to 130 g, was rapidly removed and carefully minced with scissors. Four volumes of HMS buffer (2 mM HEPES [pH 7.4], 220 mM mannitol, 70 mM sucrose) was added, and homogenization was carried out with a motor-driven Teflon pestle in a glass tissue grinder at a speed of 1,000 rpm. The homogenate was centrifuged for 1 min at $5,000 \times g$; the supernatant was collected and centrifuged at $10,000 \times g$ for 6 min. Contamination of mitochondria by lysosomes was minimized by treating the pellet with a diluted digitonin solution, according to the procedure of Loewenstein et al. (32). The final mitochondrial pellet was resuspended in HMS at a protein concentration of 20 mg/ml.

Yeast mitochondria were isolated from [*CEN-MIP1-c-myc*]-complemented cells, as described above, and resuspended in mitochondrial import buffer (0.6 M sorbitol, 50 mM HEPES-KOH [pH 7.4], 50 mM KCl, 10 mM MgCl_2 , 2 mM KH_2PO_4 , 2.5 mM EDTA, 2 mM ATP, 1 mg of BSA per ml) at a protein concentration of 40 mg/ml.

YMIP or YMIP-*c-myc* translation mixture (6 μl) was incubated with 4 μl of a suspension of freshly isolated rat liver or yeast mitochondria for 20 min at 27°C . After import, aliquots were treated with trypsin, plus or minus 1% Triton X-100, as described above. Import reactions were also separated into pellets and supernatants by centrifugation at $12,000 \times g$ for 5 min at 4°C , as described elsewhere (24). The products of the import reactions were analyzed directly by SDS-PAGE and fluorography.

Biochemical determinations. MPP and MIP activities were assayed in the mitochondrial subfractions with the following substrates, as described before (24, 25): *N. crassa* Rieske Fe-S protein precursor (pFe-S), *S. cerevisiae* F_1 ATPase subunit β precursor (pF $_{1\beta}$), human pOTC, and methionine intermediate OTC (M-iOTC; in this protein, an initiator methionine has been substituted for the phenylalanine normally present at the iOTC amino terminus). The corresponding cDNAs were transcribed in vitro, and mRNAs were translated in the presence of [^{35}S]methionine, as described above. Processing reactions were carried out for 30 min at 27°C in a final volume of 10 μl , containing 1 μl of translation mixture, 1 mM MnCl_2 , 10 mM HEPES-KOH (pH 7.4), 1 mM dithiothreitol, and 2.5 μg of total protein from the mitochondrial subfractions, and ana-

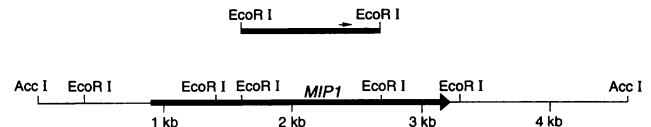


FIG. 1. Partial restriction map of *MIP1* and flanking sequences. An internal 1.1-kbp *EcoRI-EcoRI* *MIP1* gene fragment is shown in the upper part of the figure. The position of the primer complementary to the zinc-binding site coding sequence, used for initial characterization of *MIP1*, is indicated by the arrow above this fragment. An overlapping 4.6-kbp *AccI-AccI* fragment, containing the entire *MIP1* gene plus 3' and 5' flanking sequences, is shown in the lower part of the figure. *MIP1* is indicated as the solid arrow. The *EcoRI-EcoRI* restriction fragments used for sequencing the entire 4.6-kbp fragment are indicated.

lyzed directly by SDS-PAGE. The amounts of the processing reaction products were determined by densitometric analysis of fluorograms and used as a measure of MPP or MIP activity. Fumarase activity was assayed as described by Stitt (48).

Respiratory activities were determined on *mip1* or wild-type mitochondria with a multicomponent analysis used for clinical diagnosis of mitochondrial enzyme deficiency myopathies (9), consisting of six spectrophotometric enzyme assays. Cytochrome *c* oxidase activity was measured by the rate of oxidation of cytochrome *c* (55), succinate-cytochrome *c* reductase activity was measured by the rate of reduction of cytochrome *c* in the presence of succinate (49), rotenone-sensitive NADH cytochrome *c* reductase activity was measured by the rate of cytochrome *c* reduction in the presence of NADH and rotenone (18), NADH dehydrogenase activity was measured by the rate of oxidation of NADH in the presence of artificial electron acceptor ferricyanide and NAD formation (30), succinate dehydrogenase activity was measured by the rate of oxidation of succinate in the presence of artificial electron acceptor 2,6-dichlorophenol-indophenol (DCIP) (58), and citrate synthase activity was measured by the rate of condensation of acetyl-coenzyme A with oxaloacetate to form citrate and free coenzyme A (47).

Nucleotide sequence accession number. The nucleotide sequence of *MIP1* (see Fig. 2) has been deposited in GenBank under accession number U10243.

RESULTS

Two yeast genes, *YCL57w* and *MIP1*, are homologous to RMIP. The full-length RMIP cDNA was used as a probe to screen a λ DASH *S. cerevisiae* genomic library under low-stringency conditions, and 30 positive plaques were isolated from the primary screening. RMIP cDNA and *YCL57w* have 56% identity over 106 bp in the zinc-binding site coding region localized toward the 3' ends of both genes (26). This might be sufficient for hybridization of the RMIP cDNA probe to any clones containing the *YCL57w* sequence. To identify such clones, PCR amplifications were performed directly on the λ phage DNA from the 30 primary plaques, and the 3' half of *YCL57w* was specifically amplified from five of them (data not shown). The remaining 25 positive plaques might represent clones containing a gene (or genes) different from *YCL57w*. Nine clones were recovered after tertiary screening; restriction analysis indicated that they contained three overlapping inserts ranging from 15 to 18 kbp. An internal *EcoRI* fragment of about 1.1 kbp (Fig. 1) was initially isolated from one of these clones on the basis of its ability to hybridize to a RMIP cDNA probe when high-stringency conditions were used. This frag-

AGAGAGAAAAATCATATATAGCGTCAAATCAAACAATCATGAATTTACTGCAAAGACTAAATGTGTAAGGGAAATAGGTATCAGAACATTAA 96
 GTGAAGGCCCGAAGTAATATCAGTAATGCCTCGCACGATAATATTGAAAGCCGGGTCCAATGCCTCCATACCGTACACCTCCCGCCAAAATAAG 192
 M L R T I I L K A G S N A S I P S P S R Q N K 23
 T T A C T C A G G T T C T T C G C C A C A G C C G C G C A G T C T C T A G G A C C A G T C C A G G A A G C A T T T A A G A A G A T T T T C G A C G A C A A T T C A T T T G G A G A A A T T 288
 L L R F F A T A G A V S R T S P G S I K K I F D D N S Y W R N I 55
 A A T G G T C A G G A T G C T A A T A T A G C A A G A T C T C A C A A T A T C T T T T A A A A A A A A A A A A C C G G A C T T T C A A G A A C C C T T A T T T G A C T T C C A G A T 384
 N G Q D A N N S K I S Q Y L F K K N K T G L F K N P Y L T S P D 87
 G G T T T C C G T A A G T T A G C C A G G T T C T T T G C A G C A A G C A A G A A C T T C G C A A A A T G A G G A A T G A T T T T A G C G A G A T G G T A A A T T A A C C T A T 480
 G L R K F S Q V S L Q Q A Q E L L D K M R N D F S E S G K L T Y 119
 A T T A T G A A C C T G G A C A G A T T A A G C G A T A C G C T A T G T C G A G T T A T T G A T T T G T G C G A G T T A T T A G G T C A A C A C A T C C A G A T G A T G C A T T G T T A G G 576
 I M N L D R L S D T L C R V I D L C E F I R S T H P D D A F V R 151
 G C A G C A C A A G A T T G C C A T G A C A A A T G T T G A A T T C A T G A A T G T C T T G A A C A C T G A T G T T T C C T T A T G T A A C A T A C T A A A G T C G G T T T T A A A C A A T 672
 A A Q D C H E Q M F E F M N V L N T D V S L C N I L K S V L N N 183
 C C A G A A G T G T C T T C G A A G T T A A G C C G A A G A A C T T A A A G T T G G T A A A A T A T T A T T T G G A T G A T T T T G A A A A G T C A G G A A T C T A T A T G A A T C C A G A T 768
 P E V S S K L S A E E L K V G K I L L D D F E K S G I Y M N P D 215
 G T T A G A A A A G T T A T C C A G T T A T C T C A G G A A A T C A G T T A G T A G G T C A A G A A T T C A C A C C A T A C A G A C T A T C C T G G T T C A A A T T C T G T G A A G 864
 V R E K L F S Q E I S L V G Q E F I N H T D Y P G S N S V K 247
 A T A C C A T G T A A A G A T C T G G A T A A T A G T A A A G T A G T A C A T T C T A T T G A G C A A T T A A A T A A A G A T G T A A A G G G C A A A A T T A A A G T C T A C T A C A 960
 I P C K D L D N S K V S T F L L K Q L N K D V K G Q N Y K V P T 279
 T T T G G T A T G C A G C T T A T C A T T A T T A A A A G T T G T G A A A T G A G A T G T A A G A A A A A G T T G T G G A C C G C T C T C A C A G T T G T T C G A C A A A C A G 1,056
 F G Y A A Y A L K S C E N E M V R K K L L W T A L H S C D L K Q 311
 G T T A A A G A T T G A G T C A T T A T C A A A C T A A G G G C A A T C T T G G C T A A T T A A T G C C A A A A C A A G T T A C C G A G A T A T C A A T T G G A A G G T A A A A T G 1,152
 V K R L S H L I K L R A I L A N L M H K T S Y A E Y Q L E G K M 343
 G C A A G A A T C C G A A A G T T T C A A G A T T T A T T T T A G C G T T A A T G A A C A A T A C T A T A G A G A A G A C A G C A A A T G A A T T G A A A T T T A A G A A T T T A A G A C T C 1,248
 A K N P K D V Q D F I L T L M N N T I E K T A N E L K F I A E L 375
 A A G C C A A A G A T T A A G A A G C C G T T G A C T A C A A C C G G A C G A A A T T A G A A A T C G T G A G A C C A T G G G A T A G G A T T A C T A T A T G G C C A A A T A T 1,344
 K A K D L K K P L T T N T D E I L L K L V R P W D R D Y Y T G K Y 407
 T T C C A G C T C A A C C C G T C A A A C T C C C A A T G C C A A A G A A A T A A G C T A T T A T T T T A C A T T A G G A A A T G C A T T C A G G C C T T G T C A G A T T T T T C A G 1,440
 F Q L N P S N S P N A K E I S Y Y F T L G N V I Q G L S D L F Q 439
 C A A A T A T A T G G T A T T A G A T T A G A C C A G A A T T A C T G A T G A G G G A A A C A T G T C C C C A G A C G T G A G A A G A T T G A A T G T A T C T G A A G A G G A A 1,536
 Q I Y G A I R L E F A I T D E G E T W S P D V R R R L N V I S E E E 471
 G G A T C A T C G C C A T A A T T A T T G T G A T T A T T C G A A C G A A A T G G C A A G A C T T C A A A T C C G G C T C A T T T C A C A G T T T G T T G C T A G G C A G A T A T A T 1,632
 G I I G I I Y C D L F R N G K T S N P A H F T V C C S R Q I Y 503
 C C C A G T G A A A C T G A T T T C T C A A C C A T C C A A G T C G G T G A G A A T C C A G A C G T A C T A T T C A A T T A C C G T T A T T T C T T T G G T G T A A T T T T T C T 1,728
 P S E T D F S T I Q V G E N P D G D G T Y F Q L P V I S L V C N F S 535
 C C A A T A C T A A T C G C T T A A A A A A A G T C T T T G T T T T T T G C A G C T T A G T G A A G T T G A A A C G C T C T T C C A T G A A A T G G G A C A T G C A A T G C A C T C A A T G 1,824
 P I L I A S K K S L C F L Q L S E V E T L F H E M G H A M H S M 567
 T T A G G G A G A A C T C A T A T G C A A A C A T A A G T G G T A C A A G A T G C T A C T G A T T T T G A G A G T T A C C A A G A T C C T G A T G G A C A C T T C G C T A A G G A T 1,920
 L G R T H M Q N I S G T R C A T D F V E L P S I L M E H F A K D 599
 A T A C G A A T C T G A C A A A G A T T G G C A A A C A T T A C C G G A C T G G A G A A A C A T T C A G G C T G A T A T G T T A C A G C C C T C A T G A A A A G C A C T A A C T T C C T T 2,016
 I R I L T K I G K H Y G T G E T I Q A D M L Q R F M K S T N F L 631
 C A A A T T G T G A A A C T A C T C T C A A G C A A A G A T G G C T A T G C T G G A T C A A T C A T T T C A T G A T G A A A A A T C A T T T C T G A T A T T G A T A C T T T G A C G T T 2,112
 Q N C E C T Y S Q A K M A M L D Q S F H D E K I I S D I D N F D V 663
 G T G A A A A C T A T A G C A C T A G A A C G C G T T T A A A G T C C T A G T G G A C A G A T A T T G G T G T G G A A G A T T C G G C C A T T A T T T T G G A T A C G G V 2,208
 V E N Y Q A L E R R L K V L V D D Q S N W C G R F G H L F G Y G 695
 G C A A C T T A T A C A G C T A C T T A T T T G A T A G G A C G A T A G C T T C T A A A A T C T G G T A C G C C C T T T C G A G G A T G A T C C G T A C A G T C G A A A A A A T T G G T G A T 2,304
 A T Y Y S Y L F D R T I A S K I W Y A L F E D D P Y S R K N G D 727
 A A A T T T A A A A G C A T T A C T A A A A T G G G A G G G C T A A A G A C C C T T G G A A T G A T C G C T A G T G T T T T A G A A T G C C C C A T G C T A G A G A A A G G C G G T 2,400
 K F K K H L L K W G G L K D P W K C I A D V L E C P M L E K G G 759
 A G C G A T G C G A T T G A A T T A T T A G C A C A G T C T C A A G C T T A G A G A A C A G A G T A G G T G C T A A T C G A G G C C A T T A T T T G C C A A C G A C G C T T A T T C A T 2,496
 S D A M E F I A Q S H K S * 772
 A G C T G A A T T C T T T C A C C A A G A A A A A A A A A T T G C A T A A T C T T A A A A T A C T A A G A C C A T T A T T T A A A A G G G T C T G A A A C C A 2,579

FIG. 2. Nucleotide and deduced amino acid sequences of *MIP1*. Amino acids are denoted by the single-letter code. The star indicates the stop codon.

ment was characterized by sequencing using a degenerate primer derived from the amino acid sequence of the RMIP zinc-binding motif HEMGHAMH, on the basis of the idea that this site should be conserved between homologous genes. The DNA sequence obtained predicted a protein sequence with over 60% identity to the RMIP sequence in the zinc-binding site region (see below). An overlapping *AccI*-*AccI* fragment of about 4.6 kbp was then isolated and sequenced completely from both strands, by use of the *EcoRI* restriction fragments shown in Fig. 1 and universal and specific primers.

This fragment contains three open reading frames, only one of which is complete. The complete open reading frame, *MIP1*, consists of 2,316 bp specifying a primary translation product of 772 amino acids with a predicted molecular mass of 85,030 Da (Fig. 2). We have designated the *MIP1* gene product YMIP. The 37-residue amino-terminal sequence of YMIP contains six basic amino acids, no acidic residues, and predominantly hydrophobic and hydroxylated amino acids, characteristics that are typical of mitochondrial targeting signals (16). Not including the leader peptide, the YMIP protein contains a predominance of acidic (Asp and Glu) over basic (Arg and Lys) amino acids (94 versus 88), and it is generally hydrophilic.

Over its entire length, YMIP bears 31% identity and 54% similarity to RMIP. In comparison, the predicted YCL57w protein shows 24% identity and 47% similarity to RMIP. A typical zinc-binding motif, HEXXH, is localized toward the

carboxyl termini of these proteins (Fig. 3). RMIP and YMIP share the sequence LFHEMGMHAMHSLGRT, centered around this motif, while a lower degree of homology is found here between RMIP and YCL57w.

Chromosomal disruption of *MIP1* causes a respiration-

YMIP	VETLPH EMGH AMHSLGRTH M Q NSIGTRCA T.DFVELPSI	553
RMIP	MENLPH EMGH AMHSLGRTR YQHVTRCP T.DFAEVP SI	486
YCL57w	IVTFFH ELGH GIHDLVGNK ESRFNGPGSV PWFDFEAP SQ	505
YMIP	LMEHF AKDIR ILTKIGKHYG TGETIQADML QRFMKSTN FL	593
RMIP	LMEYF SMDYR VVSQFAKHYQ TGQPLPKAMV SRLCESK KVC	526
YCL57w	MLEF WTWKN ELINLSSHYK TGEKIPESLI NSLITK HEVN	545

FIG. 3. The putative zinc-binding site regions of RMIP and YMIP are identical. The deduced YMIP, RMIP (GenBank M96633), and YCL57w (GenBank X59720) protein sequences were aligned by use of the computer program PILEUP (University of Wisconsin Genetics Computer Group) with a gap penalty of 3 and a gap extension penalty of 0.1. A portion of the alignment in the zinc-binding site region is shown. The zinc-binding motif (H-E-X-X-H) is underlined. Identical residues between YMIP and RMIP or between YCL57w and RMIP are indicated by continuous bars; conservative replacements (D or E, K or R, L or I or V, F or Y or W, and S or T) are indicated by dots.

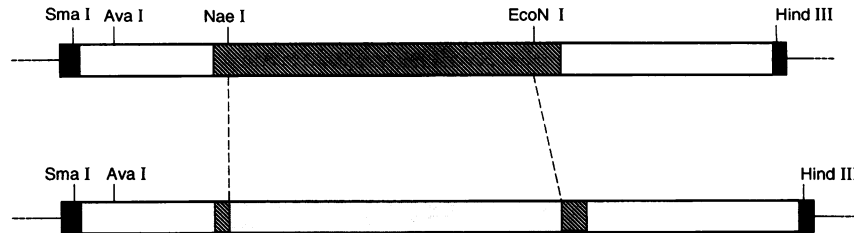

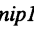
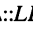
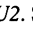


FIG. 4. Construction of the deletion allele *mip1Δ::LEU2*. See Materials and Methods for details. , *MIP1*; , *LEU2*; , *MIP1* flanking sequences; , pGEM.

deficient phenotype. For construction of a deletion allele, the internal 2,053 nucleotides coding for residues 31 to 717 of *YMIP* were deleted and replaced by the yeast *LEU2* gene (Fig. 4). The *mip1Δ::LEU2* disruption allele was substituted for one chromosomal copy of *MIP1* in diploid strains AW1-2 and YPH501. Heterozygous transformants were sporulated and, after dissection, over 30 tetrads with four viable spores were obtained (data not shown). The *mip1Δ::LEU2* disruption segregated 2+:2- on SD(-Leu); haploid cells with the disruption grew as well as the nondisrupted cells on YPD. Nondisrupted YPH501 derivatives produced a red pigment, which is typically synthesized by *ade2* strains under conditions of a normal respiratory phenotype (44). In contrast, cells with the *mip1Δ::LEU2* disruption were completely devoid of red pigmentation, which is consistent with loss of respiratory competence. This was confirmed by the inability of these mutants to grow on YPEG (data not shown). Southern blotting performed on genomic DNA isolated from respiration-deficient mutants showed a restriction pattern consistent with the presence of the *mip1Δ::LEU2* allele in these mutants (data not shown). *mip1* disruption strains, derivatives of YPH501, were used for subsequent studies.

The *mip1* disruption phenotype can be complemented by a *CEN* plasmid-encoded *YMIP* protein. For complementation of *mip1Δ::LEU2* mutants, *MIP1* was subcloned into a *CEN* plasmid bearing the yeast *URA3* gene. This construct was introduced via transformation into a heterozygous disruption strain carrying the wild-type *MIP1* and *mip1Δ::LEU2* alleles. After sporulation and dissection of 11 tetrads, 9 tetrads with four viable spores were obtained (data not shown). The *mip1Δ::LEU2* disruption segregated 2+:2- on SD(-Leu); nine disruption spores appeared to have acquired a *CEN* plasmid copy of *MIP1* by their ability to grow on SD(-Ura -Leu) and were complemented for red pigment formation on YPD and for normal growth on YPEG (data not shown). An identical procedure was followed for construction of *mip1* strains complemented by a *MIP1-c-myc* fusion gene, coding for a chimeric protein with a carboxyl-terminal *c-myc* (9E10) epitope, as described in Materials and Methods. The growth rates of wild-type, mutant, and complemented cells were tested in liquid YPEG for over 40 h at 30°C (data not shown). While essentially no growth was observed for three independent *mip1* strains, three [*CEN-MIP1*]- and three [*CEN-MIP1-c-myc*]-complemented strains grew as well as wild-type cells, confirming that the respiration-deficient phenotype of *mip1* mutants is caused by loss of a functional *MIP1* gene and also indicating that the *c-myc* epitope tagging of *YMIP* does not have any deleterious effects on the function of this protein.

The Fe-S and CoxIV intermediates are not processed to mature-size proteins in *mip1* cells. In *S. cerevisiae*, the presequences of Fe-S and CoxIV precursor proteins are processed in two steps through an octapeptide-containing intermediate

(6, 12, 15, 22). If *MIP1* encodes the yeast homolog of RMIP, formation of mature Fe-S and mature CoxIV should be blocked in *mip1*- and restored in [*CEN-MIP1*]-complemented cells.

We performed immune blotting on total cell extracts prepared from these strains and wild-type cells. The temperature-sensitive mutants *mif1* and *mif2*, which accumulate uncleaved precursors at 37°C because of defects in the general matrix protease MPP (35, 57), were also used for the migration positions of precursor species.

The intermediate (iFe-S) and mature forms of yeast Fe-S can normally be detected by immune blotting of mitochondrial membranes or the purified *bc₁* complex, while precursor Fe-S (pFe-S) is generally not detected in yeast mitochondria under steady-state growth conditions (15). Our results are consistent

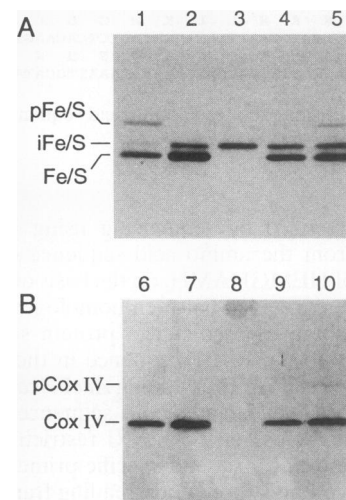


FIG. 5. *mip1* mutant cells cannot form mature Fe-S and mature CoxIV subunits. Fe-S (A) and CoxIV (B) immune blotting was performed on total cell extracts from wild-type (lanes 2 and 7), *mip1* (lanes 3 and 8), [*CEN-MIP1*]-complemented (lanes 4 and 9), and temperature-sensitive *mif1* (lanes 1 and 6) and *mif2* (lanes 5 and 10) cells, as described in Materials and Methods. Cells were grown in YPD at 30°C to an OD_{600} of 1. The temperature-sensitive mutants *mif1* and *mif2* were grown for 12 h at room temperature and then shifted to the nonpermissive temperature for 90 min. For Fe-S detection, a mouse anti-yeast Fe-S monoclonal antibody was used, while a rabbit anti-yeast CoxIV serum was used for CoxIV analysis. The migration positions of precursor- (pFe-S and pCoxIV), intermediate- (iFe-S), and mature-size (Fe-S and CoxIV) species are indicated. The migration positions of mature Fe-S and mature CoxIV were confirmed by the migration positions of the molecular weight (MW) markers trypsin inhibitor (MW, 21,500) and lysozyme (MW, 14,300), respectively.

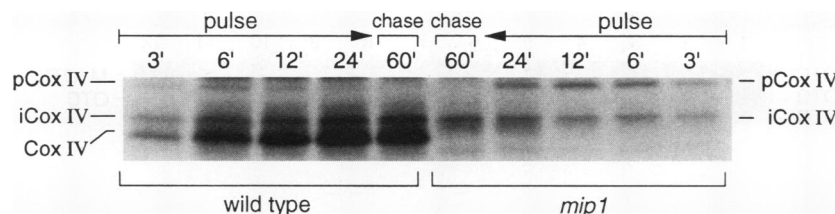


FIG. 6. Uncleaved iCoxIV accumulates in pulse-labeled *mip1* cells. Wild-type and *mip1* cells were grown in SD medium containing the appropriate growth requirements to an OD_{600} of 1 and labeled with 0.1 mCi of $Tran^{35}S$ -Label per ml for 24 min at 30°C. Labeling was stopped by addition of 0.5% unlabeled methionine and 0.5% unlabeled cysteine, and the cells were chased at 30°C for 60 min. Aliquots (1 ml) were withdrawn at the indicated time points, and immunoprecipitation was carried out on total cell extracts with an anti-yeast CoxIV serum, as described in Materials and Methods. The immunoprecipitated radiolabeled products were analyzed by SDS-PAGE and fluorography.

with these previous observations. iFe-S and mature Fe-S were detected in wild-type cells (Fig. 5A, lane 2). Conversion of iFe-S to mature Fe-S was blocked in *mip1* cells (Fig. 5A, lane 3), as indicated by the absence of mature Fe-S and accumulation of iFe-S. Formation of mature Fe-S was restored in [*CEN-MIP1*]-complemented cells (Fig. 5A, lane 4). In *mif1* (Fig. 5A, lane 1) and *mif2* (lane 5) mutants, unprocessed precursor, accumulated during 90 min of incubation at the nonpermissive temperature, indicated the migration position of pFe-S relative to the positions of iFe-S and mature Fe-S.

In immune blotting of total yeast cell extracts, mature CoxIV alone is observed, while precursor (pCoxIV) and intermediate (iCoxIV) forms are not detected under steady-state growth conditions (10, 21). Consistent with these previous observations, only mature CoxIV was detected in wild-type cells (Fig. 5B, lane 7). A lack of any immune-detectable CoxIV species characterized the *mip1* mutant (Fig. 5B, lane 8), while mature CoxIV formation was restored in [*CEN-MIP1*]-complemented cells (lane 9). *mif1* (Fig. 5B, lane 6) and *mif2* (lane 10) mutants showed the migration position of uncleaved pCoxIV relative to the position of mature CoxIV; no iCoxIV was detected in these mutants.

Because pCoxIV and iCoxIV species can be detected, along with mature CoxIV, in *in vivo* labeling experiments (21), it should be possible to detect accumulation of newly synthesized iCoxIV in pulse-labeled *mip1* cells. For this experiment, wild-type and mutant cells were labeled for 24 min and then chased for 60 min at 30°C. Aliquots were withdrawn from the cell cultures at different time points, and the radiolabeled CoxIV products were recovered by immunoprecipitation and analyzed by SDS-PAGE (Fig. 6). In wild-type cells, mature CoxIV accumulated over 24 min of labeling. In *mip1* cells, formation of mature CoxIV was blocked, while pCoxIV and iCoxIV species accumulated over the entire duration of the labeling. At the end of a 60-min chase, pCoxIV was no longer detected, while iCoxIV was recovered in an amount corresponding to approximately 50% of the total amount of precursor plus intermediate forms present at the start of the chase period.

Taken together, these results indicate that, in wild-type cells, iCoxIV is rapidly processed to mature CoxIV, such that the amounts of this intermediate are too small to be detected in a total cell extract at steady state. They further indicate that, in *mip1* cells, the uncleaved iCoxIV is rapidly degraded, in contrast with the apparent higher stability of iFe-S. The data regarding iCoxIV are similar to results obtained in cultured HeLa cells stably transformed with the human pOTC cDNA, in which pOTC and iOTC can be detected by radiolabeling and immunoprecipitation, and not by immune blotting (23), consistent with further observations that *in vivo*-synthesized radiolabeled iOTC cannot assemble into trimeric native OTC (22a).

As a control, we also analyzed cytochrome c_1 processing. This precursor is normally processed to mature c_1 in two steps by MPP and a different second peptidase, inner-membrane protease, in the intermembrane space (33, 52). Mature cytochrome c_1 formation was not altered in *mip1* disruption cells, indicating that the disruption specifically affects the MIP-dependent two-step processing pathway (Fig. 7).

***mip1* mitochondrial subfractions cannot process human iOTC to mature-size protein.** We have shown previously that human pOTC is cleaved in two sequential steps by purified rat liver MPP and MIP *in vitro*, via formation of an octapeptide-containing intermediate; moreover, an artificial intermediate OTC protein (M-iOTC), translated *in vitro* from a methionine that substitutes for the phenylalanine normally at the iOTC octapeptide amino terminus (24, 25), was shown to be processed to mature OTC by highly purified RMIP independently of the presence of MPP (28). We have analyzed processing of these substrates *in vitro* with crude soluble (representing matrix plus intermembrane space) and membrane (representing inner plus outer membrane) fractions, prepared from *mip1* and wild-type yeast mitochondria, as described in Materials and Methods. *In vitro*-translated substrates were incubated with identical amounts of total protein from each of these fractions (normally, 5 μ g) for 30 min at 27°C, under conditions established before for *in vitro* processing with rat liver MPP and/or MIP (24, 25, 28). Formation of iOTC and mature-size OTC was detected upon incubation of pOTC with a crude rat liver mitochondrial soluble fraction (Fig. 8A, lane 2). Similarly, although less efficiently, iOTC and OTC were formed upon incubation of pOTC with a wild-type yeast mitochondrial soluble fraction (Fig. 8A, lane 3). A much lower conversion of pOTC to iOTC was detected upon incubation with a wild-type yeast mitochondrial membrane fraction, leading to formation of very small amounts of mature-size OTC (Fig. 8A, lane 4).

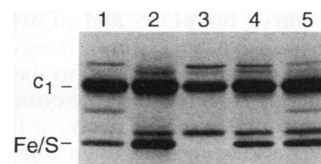


FIG. 7. Maturation of cytochrome c_1 is not affected in *mip1* cells. The same blot used for Fe-S detection (Fig. 5A) was reprobed with a mouse anti-yeast c_1 monoclonal antibody, as described in the legend for Fig. 5. Results from wild-type (lane 2), *mip1* (lane 3), and [*CEN-MIP1*]-complemented (lane 4) cells and from temperature-sensitive *mif1* (lane 1) and *mif2* (lane 5) cells are shown. The migration positions of mature c_1 and mature Fe-S are indicated.

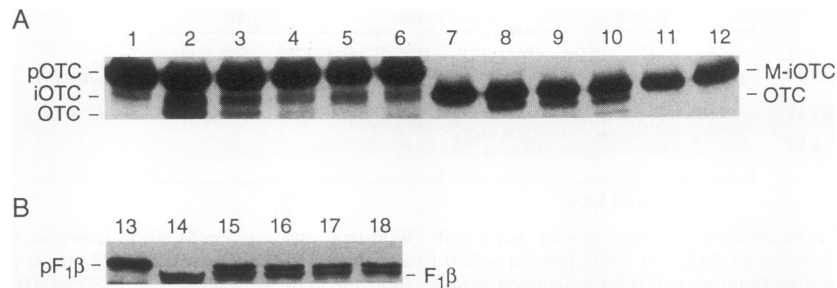


FIG. 8. *mip1* mitochondria contain normal MPP activity but are devoid of MIP activity. Mitochondria were isolated from wild-type and *mip1* cells grown in YPGal, resuspended in MIB (500 μ l at 20 mg/ml), subjected to sonication at 0 to 4°C (three 45-s pulses at 20 W with three 1-min intervals), and separated into supernatant (representing matrix plus intermembrane space) and pellet (representing inner plus outer membrane) by centrifugation at 165,000 \times g for 30 min at 4°C. Pellets were resuspended in the same volume of MIB as the supernatants, and total protein concentrations were assayed in each fraction by the Bradford procedure (4). Radiolabeled human pOTC and M-iOTC (this intermediate is translated from a methionine that substitutes for the amino-terminal phenylalanine in the normal iOTC), and *S. cerevisiae* pF₁β were synthesized by coupled in vitro transcription/translation. Processing reaction mixtures contained 1 μ l of pOTC (A, lanes 1 to 6), M-iOTC (lanes 7 to 12), or pF₁β (B) translation mixtures and 5 μ g of total protein from either the wild-type soluble (lanes 3, 9, and 15) and membrane (lanes 4, 10, and 16) fractions or the *mip1* soluble (lanes 5, 11, and 17) and membrane (lanes 6, 12, and 18) fractions, in a final volume of 10 μ l of 10 mM HEPES-KOH (pH 7.4)–1 mM dithiothreitol–1 mM MnCl₂. A rat liver soluble mitochondrial fraction was used in control reactions (lanes 2, 8, and 14). Incubations were carried out at 27°C for 30 min, and the reactions were analyzed directly by SDS-PAGE and fluorography.

Although we could detect processing of pOTC to iOTC by both the soluble (Fig. 8A, lane 5) and membrane (lane 6) *mip1* mitochondrial fractions, iOTC was not processed to mature-size OTC by these fractions. Essentially identical results were obtained when the *N. crassa* pFe-S, also known to be cleaved in two steps (17) and previously shown to be processed in vitro by rat liver MPP and MIP (24), was used as the substrate (data not shown).

With both wild-type and *mip1* mitochondrial subfractions, processing of human pOTC and *N. crassa* pFe-S was not as efficient as processing of yeast pF₁β (see Fig. 8B, below). Because mature-size OTC and Fe-S formation by MIP is dependent upon initial cleavage of the corresponding precursors by MPP (24), we further tested for the presence of MIP activity in *mip1* mitochondria using M-iOTC (Fig. 8A, lane 7) as the substrate. Formation of significant amounts of mature-size OTC was detected upon incubation of M-iOTC with both the soluble (Fig. 8A, lane 9) and membrane (lane 10) fractions from wild-type yeast mitochondria. In contrast, M-iOTC was not processed by either of the *mip1* mitochondrial fractions (Fig. 8A, lanes 11 and 12), strongly supporting the conclusion that MIP1 encodes a functional homolog of RMIP. On the other hand, pF₁β (Fig. 8B, lane 13), normally processed in one step by MPP alone (24, 53), was efficiently processed to mature-size F₁β by the soluble and membrane fractions from both wild-type (lanes 15 and 16) and *mip1* mitochondria (lanes 17 and 18), confirming that the MIP-dependent two-step processing pathway is specifically affected in *mip1* mitochondria.

YMIP is not required for pFe-S and pCoxIV import into mitochondria in vivo. It has been shown before that the Fe-S and CoxIV subunits are initially targeted to the mitochondrial matrix and subsequently assemble into the cytochrome *bc*₁ and cytochrome oxidase complex, respectively, in the inner membrane (10, 17). It has also been shown that conversion of iFe-S to mature Fe-S normally occurs after iFe-S is assembled in the cytochrome *bc*₁ complex and that iFe-S is normally present in this complex (15).

We have analyzed whether the unprocessed iFe-S and iCoxIV proteins which accumulate in *mip1* cells remain soluble in the mitochondrial matrix or are targeted to the inner membrane in vivo. Mitochondria isolated from wild-type and

mip1 disruption cells were treated with trypsin to digest any membrane-bound or incompletely imported precursors and subsequently fractionated into soluble and membrane fractions, by sonication at 4°C followed by high-speed centrifugation. This fractionation procedure was chosen because it does not involve the use of detergents and because it should be rapid enough to prevent complete degradation of any unprocessed iCoxIV accumulated in *mip1* mitochondria at steady state. When trypsin-treated *mip1* mitochondria were analyzed, both iFe-S and iCoxIV were protected from externally added protease (Fig. 9, lanes 4 and 10, respectively) but became protease accessible when trypsin treatment was performed in the presence of 1% Triton X-100 (data not shown). Upon fractionation of trypsin-treated wild-type mitochondria, over 70% of iFe-S and mature-size Fe-S proteins were localized, as expected, to the membrane fraction (Fig. 9A, lane 3), while less than 30% was found in the soluble fraction (lane 2). In *mip1* mitochondria, partitioning of uncleaved iFe-S between soluble (Fig. 9A, lane 5) and membrane (lane 6) fractions paralleled that of iFe-S and mature Fe-S in wild-type mitochondria, suggesting that the unprocessed iFe-S had been normally targeted to the inner membrane. Over 70% of mature-size CoxIV protein was found in the membrane fraction from wild-type mitochondria, and no iCoxIV protein was detected (Fig. 9B, lane 9). Small amounts of unprocessed iCoxIV could be detected in *mip1* mitochondria; most of this intermediate was found in the supernatant (Fig. 9B, lane 11), and less than 30% was found in the membrane fraction (lane 12), a distribution opposite to that of mature CoxIV and similar to the distribution of fumarase, a soluble mitochondrial matrix enzyme (Fig. 9C).

YMIP is required for normal respiratory chain function. The lack of maturation of iFe-S and iCoxIV might affect the biogenesis of complex III and complex IV of the respiratory chain, respectively, which would explain the inability of *mip1* mutants to utilize nonfermentable substrates for growth. Respiratory activities were assayed in wild-type and *mip1* mitochondria (Table 1). Mutant mitochondria were devoid of cytochrome *c* oxidase activity, indicating a lack of function of complex IV. Further, they exhibited a complete deficiency of succinate-cytochrome *c* reductase activity and a 72% reduction of rotenone-sensitive NADH cytochrome *c* reductase activity,

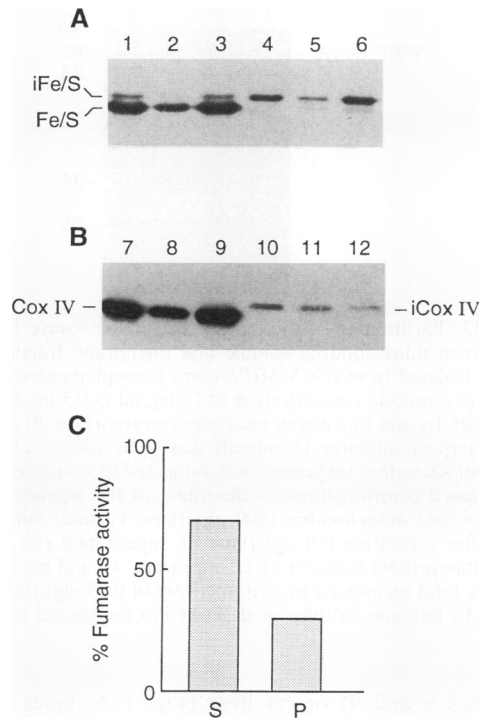


FIG. 9. YMIP is not required for pFe-S and pCoxIV import in vivo. Mitochondria were isolated from wild-type and *mip1* cells, resuspended in MIB at 20 mg of protein per ml, and treated with trypsin (0.4-mg/ml final concentration) for 5 min on ice, followed by soybean trypsin inhibitor (1-mg/ml final concentration). Soluble and membrane fractions were prepared from trypsin-treated mitochondria, as described in the legend for Fig. 8. Fe-S (A) and CoxIV (B) proteins were detected by immune blotting, as described in the legend for Fig. 5. Samples (50 μ g) of trypsin-treated mitochondria from wild-type (lanes 1 and 7) or *mip1* (lanes 3 and 10) cells were analyzed. Amounts of protein corresponding to 1% of the total protein recovered in either the wild-type soluble (lanes 2 and 8) and membrane (lanes 3 and 9) fractions or the *mip1* soluble (lanes 5 and 11) and membrane (lanes 6 and 12) fractions were analyzed. Fumarase activity (C) was assayed in wild-type and *mip1* soluble (S) and membrane (P) fractions by the method of Stitt (48) and is expressed as a percentage of the total activity recovered in these fractions.

consistent with a defect at the level of complex III, as a fault here would impair oxidation of both reduced flavin adenine dinucleotide (FADH)-linked and NADH-linked substrates. A 66% reduction of NADH dehydrogenase activity and a 90% reduction of succinate dehydrogenase activity were also detected in the mutant mitochondria, while citrate synthase activity was normal.

YMIP is imported to the mitochondria and predominantly behaves as a soluble matrix protein. When the *MIP1* gene and the *MIP1-c-myc* fusion gene were transcribed and translated in vitro, a major product of about 85 kDa was obtained in both

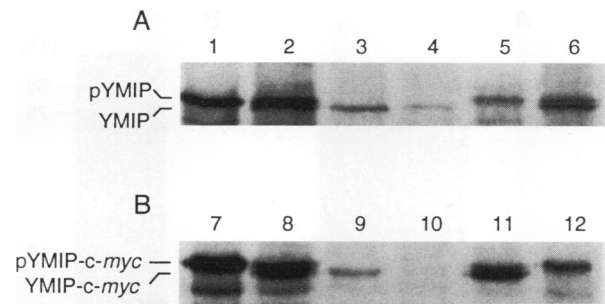


FIG. 10. The YMIP and YMIP-*c-myc* precursors are imported by isolated mitochondria in vitro. (A) Six microliters of in vitro-translated pYMIP (unprocessed; lane 1) was incubated with 4 μ l of freshly isolated rat liver mitochondria in HMS buffer at 8 mg of mitochondrial protein per ml (final concentration) for 20 min at 27°C (lane 2). After import, one sample was treated with trypsin (lane 3), as described in the legend for Fig. 9. Triton X-100 (1%) was added to another sample before trypsin (lane 4). Mitochondria were also reisolated by centrifugation for 5 min at 12,000 \times g, and the resulting supernatant (lane 5) and pellet (lane 6) were analyzed separately. Import reactions were analyzed directly by SDS-PAGE and fluorography. (B) Mitochondria were isolated from [*CEN-MIP1-c-myc*]-complemented cells that had been grown in semisynthetic medium (containing 3% glycerol, 2% ethanol, and 0.05% dextrose) to an OD₆₀₀ of 1 and resuspended in import buffer (0.6 M sorbitol, 50 mM HEPES-KOH [pH 7.4], 50 mM KCl, 10 mM MgCl₂, 2 mM KH₂PO₄, 2.5 mM EDTA, 2 mM ATP, 1 mg of BSA per ml). Six microliters of in vitro-translated pYMIP-*c-myc* (unprocessed; lane 7) were incubated with 4 μ l of this mitochondrial suspension at 16 mg of mitochondrial protein per ml (final concentration) for 20 min at 27°C (lane 8). After import, identical samples were treated with trypsin (lane 9) or 1% Triton X-100 and trypsin (lane 10) or separated into pellet (lane 11) and supernatant (lane 12), as described above. The 75-kDa band is visible immediately below the mature-size YMIP-*c-myc* band.

cases, the *MIP1-c-myc* product presenting a slightly lower mobility, consistent with the presence of the *c-myc* epitope at the protein carboxyl terminus (data not shown). To analyze the intramitochondrial localization of YMIP, the putative YMIP and YMIP-*c-myc* precursors were initially incubated with freshly isolated rat liver or yeast mitochondria, under conditions established before for import of the RMIP precursor (26). pYMIP (Fig. 10A, lane 1) was processed by rat liver mitochondria to a smaller product likely to represent mature-size YMIP (lane 2). This product was protected from externally added trypsin (Fig. 10A, lane 3), but mostly became protease accessible when trypsin treatment was performed in the presence of 1% Triton X-100 (lane 4). When the mitochondria were reisolated by centrifugation after import, most of the unprocessed pYMIP remained in the supernatant (Fig. 10A, lane 5), while mature YMIP sedimented with the mitochondrial pellet (lane 6). Essentially identical results were obtained when in vitro-translated pYMIP-*c-myc* was incubated with mitochondria isolated from [*CEN-MIP1-c-myc*]-comple-

TABLE 1. Respiratory activities of wild-type and *mip1* mitochondria

Source of mitochondria	Sp act (μ mol/min/mg) of:					
	Cytochrome oxidase	Succinate- <i>c</i> reductase	NADH- <i>c</i> reductase	Succinate dehydrogenase	NADH dehydrogenase	Citrate synthase
Wild type	6.41	0.93	2.56	5.00	30.46	12.43
<i>mip1</i>	0.07	0.01	0.72	0.52	13.41	12.43

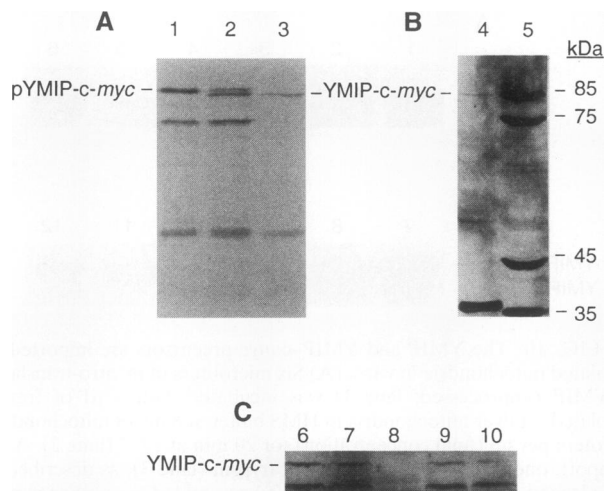


FIG. 11. A YMIP-*c-myc* fusion protein is imported to the mitochondria in vivo. (A) In vitro-translated pYMIP-*c-myc* (unprocessed; lane 1) was incubated with freshly isolated rat liver mitochondria (lane 2), and trypsin treatment was carried out upon import (lane 3), as described in the legend for Fig. 10. (B) A sample treated identically to the sample shown in panel A, lane 3 (lane 4), and a sample containing 500 μ g (total protein) of a mitochondrial suspension from [*CEN-MIP1-c-myc*]-complemented cells (lane 5) were analyzed by immune blotting, with a *c-myc* epitope (9E10) mouse monoclonal antibody. (C) Freshly isolated mitochondria from [*CEN-MIP1-c-myc*]-complemented cells were adjusted to a protein concentration of 20 mg/ml in MIB. Aliquots (60 μ l) were analyzed without further treatment (lane 6) or were treated with trypsin (lane 7) or 1% Triton X-100 and trypsin (lane 8). Mitoplasts were prepared by dilution of the mitochondria with 5 volumes of 20 mM HEPES-KOH (pH 7.4) for 10 min on ice and agitation on a Vortex mixer, followed by centrifugation at 12,000 \times *g* for 5 min at 4°C, and analyzed directly (lane 9) or after trypsin treatment (lane 10), as above. In fluorograms A, B, and C, the 75-kDa band is visible below the mature-size YMIP-*c-myc* band.

mented cells (Fig. 10B, lanes 7 to 12) or with rat liver mitochondria (Fig. 11A, lanes 1 to 3). Consistent with normal growth of [*CEN-MIP1-c-myc*]-complemented cells on YPEG, these results indicate that *c-myc* epitope tagging of YMIP does not affect mitochondrial targeting of this protein.

We then analyzed the intramitochondrial localization of the YMIP-*c-myc* fusion protein in vivo. A sample containing in vitro-translated pYMIP-*c-myc* precursor (Fig. 11A, lane 1) that had been imported into isolated rat liver mitochondria (lane 2) and subsequently treated with trypsin (lane 3) was analyzed by immune blotting (Fig. 11B, lane 4) at the same time as 500 μ g of mitochondria (total protein) isolated from [*CEN-MIP1-c-myc*]-complemented cells (lane 5), by use of a mouse monoclonal anti-*c-myc* epitope (9E10) antibody (11). In yeast mitochondria (Fig. 11B, lane 5), an 85-kDa protein with the same electrophoretic mobility as the mature-size YMIP-*c-myc* protein formed by isolated rat liver mitochondria (lane 4) was detected. Three additional bands, of 75, 45, and 35 kDa, were also detected in yeast mitochondria (Fig. 11B, lane 5). Neither the 85-kDa protein nor these other bands were detected in the cytosolic fraction or in a total cell extract from cells complemented by a nonfusion *MIP1* gene (data not shown). A 75-kDa band was also present in the pYMIP-*c-myc* in vitro translation mixture (Fig. 10B, lane 1, and Fig. 11A, lane 1). Unlike the full-length pYMIP-*c-myc*, however, this shorter product was not imported or processed by isolated yeast (Fig.

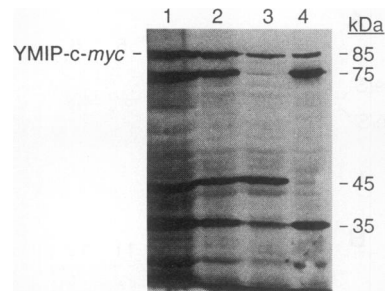


FIG. 12. Partitioning of the mature-size YMIP-*c-myc* fusion protein between mitochondrial soluble and membrane fractions. Mitochondria isolated from [*CEN-MIP1-c-myc*]-complemented cells were adjusted to a protein concentration of 50 mg/ml in 0.5 ml of MIB and treated with trypsin (0.2 mg/ml final concentration) for 20 min on ice; soybean trypsin inhibitor (1 mg/ml) was then added. The trypsin-treated mitochondrial suspension was subjected to sonication followed by high-speed centrifugation, as described in the legend for Fig. 8. Trypsin-treated mitochondria (500 μ g) (lane 1), total mitochondrial extract after sonication (50 μ g) (lane 2), supernatant (25 μ g from a total soluble protein recovery of 1.1 mg) (lane 3), and membrane (25 μ g from a total membrane protein recovery of 0.75 mg) (lane 4) were analyzed by immune blotting, as described in the legend for Fig. 11.

10B, lanes 8 and 9) or rat liver (Fig. 11A, lanes 2 and 3) mitochondria.

When aliquots (120 μ g of total protein) of the isolated yeast mitochondria (Fig. 11C, lane 6) were treated with trypsin, YMIP-*c-myc* was protected (lane 7), becoming protease accessible when trypsin treatment was performed in the presence of 1% Triton X-100 (lane 8). When mitochondria were subjected to osmotic shock and mitoplasts were reisolated by centrifugation, YMIP-*c-myc* sedimented with the pellet (Fig. 11C, lane 9) and was protected from externally added trypsin (lane 10). These data indicate that the *MIP1-c-myc* fusion gene product is imported to the mitochondria in vivo. The 75-, 45-, and 35-kDa bands also appeared to be protected from externally added trypsin, both in intact mitochondria and in mitoplasts (only the data for the 75-kDa band are shown in Fig. 11C); however, only the 75-kDa protein was fully digested by trypsin in the presence of Triton X-100 (lane 8), while about 50% of the 45-kDa protein and most of the 35-kDa protein were resistant to trypsin treatment (not shown).

To define the intramitochondrial localization of the mature-size YMIP-*c-myc* protein, isolated yeast mitochondria were treated with trypsin and subsequently fractionated by sonication and high-speed centrifugation into soluble and membrane fractions, as described above. This fractionation procedure was carried out twice with mitochondria isolated from two independent [*CEN-MIP1-c-myc*]-complemented strains, giving very similar results regarding protein recovery and specific enzymatic activities each time. In Fig. 12, trypsin-treated mitochondria (500 μ g) (lane 1), total mitochondrial extract after sonication (50 μ g) (lane 2), and soluble (25 μ g) (lane 3) and membrane (25 μ g) (lane 4) fractions were analyzed at the same time. By densitometric analysis, the amount of mature-size YMIP-*c-myc* detected in the soluble fraction was 10 to 15% higher than the amount detected in the membrane fraction. Thus, relative to the total protein recovered in the supernatant (1.1 mg) and the pellet (0.75 mg), mature YMIP-*c-myc* was found in these fractions at levels of about 60 and 40%, respectively.

The 75-kDa band was detected almost exclusively in the membrane fraction (Fig. 12, lane 4). Because the levels of specific MIP activity recovered in the soluble and membrane

fractions correlated with the amounts of mature-size YMIP-*c-myc* protein and not with the amounts of 75-kDa protein (see below), the 75-kDa band may not have any functional significance; it may represent an abnormal transcription/translation product of the *CEN* plasmid-encoded *MIP1-c-myc* fusion gene which is incompletely imported. The 45- and 35-kDa bands appear to represent carboxyl-terminal products of some proteolytic cleavage(s) within the 85- and 75-kDa proteins, respectively. The occurrence of an internal cleavage in the mature-size YMIP-*c-myc* protein would be consistent with our previous observations that a highly purified RMIP fraction also contains two peptides, of 45 and 28 kDa, resulting from a single cleavage within the full-length RMIP protein (28). This internal proteolytic cleavage is not autocatalytic and may be responsible for the rapid inactivation of RMIP in mitochondrial matrix (28).

MIP activity was measured by incubating in vitro-translated M-iOTC with identical amounts (2.4 or 0.8 μ g of total protein) of the soluble and membrane fractions used for YMIP-*c-myc* localization studies. On the basis of the amounts of mature OTC formed in 30 min at 27°C, the levels of MIP activity recovered in the soluble fraction (Fig. 13A, lanes 3 and 4) were 1.5-fold higher than those recovered in the membrane fraction (lanes 5 and 6). This result was reproduced in three independent assays. Thus, relative to the total protein recovered in these two fractions (see above), over 60% of MIP activity was soluble while about 40% was membrane associated (Fig. 13A, graph), consistent with the intramitochondrial distribution of mature-size YMIP-*c-myc* protein.

Identical conditions were used for MPP activity determination, with in vitro-translated yeast pF₁ β as the substrate. On the basis of the amounts of mature-size F₁ β produced, MPP activity was recovered in the soluble fraction (Fig. 13B, lanes 9 and 10) at a level twofold higher than in the membrane fraction (lanes 11 and 12). This result was also confirmed by three independent assays. Thus, relative to the total protein in each fraction, over 75% of MPP activity was soluble (Fig. 13B, graph). Immune blotting of mature-size Fe-S protein (Fig. 13, lanes 13 to 15 and graph) and fumarase activity determinations (Fig. 13D, graph) were also performed in the same fractions, as described above. Consistent with the hydrophilicity of the predicted YMIP sequence, partitioning of MIP activity between soluble and membrane fractions appeared to parallel the distribution of MPP and fumarase activity more closely than that of the Fe-S protein.

Construction and analysis of a strain with a disrupted copy of *YCL57w*. The genetic inactivation of *YCL57w* was carried out to exclude the possibility that this gene may encode a redundant MIP-like activity. Gene *YCL57w* was PCR amplified from genomic yeast DNA with specific primers on the basis of the published sequence of yeast chromosome III (34). The internal 1,717 bp coding for residues 92 to 663 of *YCL57w* were deleted and replaced by the yeast *LEU2* gene. This null allele was substituted for one chromosomal copy of *YCL57w* in diploid strain AW1-2. After sporulation and tetrad dissection, the presence of the *ycl57w* Δ ::*LEU2* disruption in haploid strains capable of growing on SD(-Leu) was confirmed by Southern blotting (data not shown). Haploid strains with the disrupted *ycl57w* Δ ::*LEU2* allele grew equally as well as wild-type cells both on YPD and YPEG plates (data not shown).

We also analyzed the growth phenotype of double-disruption strains, harboring a *mip1* Δ ::*LEU2* and a *ycl57w* Δ ::*URA3* allele, as described in Materials and Methods. The growth rates of wild-type, *ycl57w*, and *mip1 ycl57w* cells were tested in liquid YPD and YPEG at 30°C (data not shown). The *ycl57w* cells grew as well as wild-type cells in both media. The growth

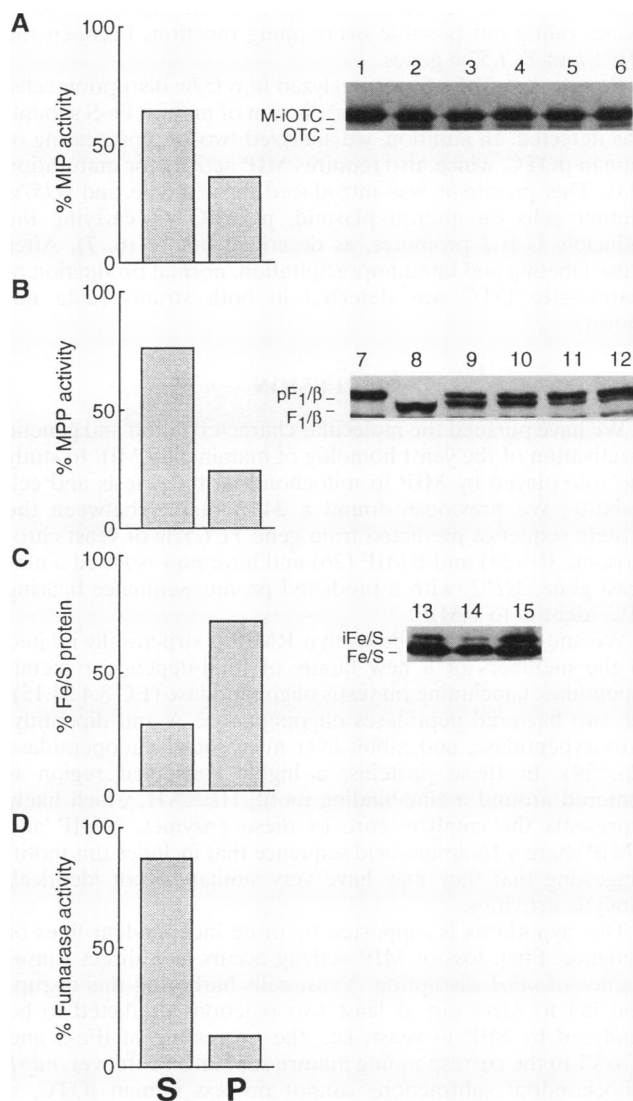


FIG. 13. Partitioning of MIP activity between mitochondrial soluble and membrane fractions. In vitro-translated M-iOTC (A, fluorogram) and pF₁ β (B, fluorogram) were incubated with the soluble (2.5 μ g [lanes 3 and 9] or 0.8 μ g [lanes 4 and 10] of total protein) and mitochondrial-membrane (2.5 μ g [lanes 5 and 11] or 0.8 μ g [lanes 6 and 12] of total protein) fractions described in the legend for Fig. 12. A rat liver mitochondrial soluble fraction was used in control reactions (lanes 2 and 8). Processing reactions were carried out and analyzed as described in the legend for Fig. 8. This experiment was repeated three times, and the amounts of mature OTC and mature F₁ β formed in different reactions were estimated by densitometry of fluorograms and used as arbitrary measures of MIP and MPP activity, respectively. The amounts of Fe-S protein in trypsin-treated mitochondria (500 μ g) (C, fluorogram, lane 13) and in the mitochondrial soluble (25 μ g) (lane 14) and membrane (25 μ g) (lane 15) fractions were measured by immune blotting and densitometry, and fumarase activity was measured by the method described by Stitt (48). The percents MIP activity (A, graph), MPP activity (B, graph), mature Fe-S protein (C, graph), and fumarase activity (D) in the soluble (S) and membrane (P) fractions relative to the total protein recovered in each of these two fractions were estimated.

phenotype of *mip1 ycl57w* cells was undistinguishable from that of *mip1* mutant cells, and, thus, the double disruption did not result in a more severe phenotype than the *mip1* disruption alone, ruling out possible overlapping functions between the *MIP1* and *YCL57w* genes.

Processing of pFe-S was analyzed in *ycl57w* disruption cells, as described above. Normal production of mature Fe-S subunit was detected. In addition, we analyzed two-step processing of human pOTC, which also requires MIP activity for maturation (24). This precursor was introduced in wild-type and *ycl57w* mutant cells on a 2 μ m plasmid, pGALOTC, carrying the inducible *GAL1* promoter, as described before (6, 7). After pulse labeling and immunoprecipitation, normal production of mature-size OTC was detected in both strains (data not shown).

DISCUSSION

We have pursued the molecular characterization and genetic inactivation of the yeast homolog of mammalian MIP to study the role played by MIP in mitochondrial biogenesis and cell viability. We previously found a 24% identity between the protein sequence predicted from gene *YCL57w* of yeast chromosome III (34) and RMIP (26) and have now isolated a new yeast gene, *MIP1*, with a predicted protein sequence bearing 31% identity to RMIP.

We and others have shown that RMIP is structurally related to the members of a new family of thiol-dependent metalloproteases, including rat testis oligopeptidase (EC 3.4.24.15), the two bacterial peptidases oligopeptidase A and dipeptidyl carboxypeptidase, and rabbit liver microsomal endopeptidase (26, 29). In these proteins, a highly conserved region is centered around a zinc-binding motif, HEXXH, which likely represents the catalytic core of these enzymes. YMIP and RMIP share a 16-amino-acid sequence that includes this motif, suggesting that they may have very similar, if not identical, catalytic activities.

This hypothesis is supported by three independent lines of evidence. First, loss of MIP activity occurs as a direct consequence of *mip1* disruption. Yeast cells harboring this disruption fail to carry out at least two reactions predicted to be catalyzed by MIP in yeast, i.e., the processing of iFe-S and iCoxIV to the corresponding mature subunits. Moreover, *mip1* mitochondrial subfractions cannot process human iOTC, a substrate specifically cleaved by RMIP (28). On the other hand, normal processing of iFe-S and iCoxIV in vivo and of human iOTC in vitro can be restored when *mip1* cells are complemented by a *CEN* plasmid-encoded YMIP protein.

A second line of evidence is provided by the fact that disruption of another sequence, having 24% identity with RMIP, i.e., *YCL57w*, does not affect MIP activity. Cells harboring this disruption show normal processing of both the endogenous pFe-S and the episomally encoded human pOTC. Also, these cells have a normal respiratory phenotype. Further, because a double *mip1 ycl57w* mutant does not present a more severe phenotype than the single *mip1* disruption mutant, it appears that there are no overlapping functions between *MIP1* and *YCL57w*. It has recently been proposed that *YCL57w* may encode the cytosolic and mitochondrial forms of the yeast protease yscD (50), an 83-kDa thiol-dependent metalloprotease previously characterized in *S. cerevisiae* (13). Consistent with our observations in *ycl57w* disruption cells, yeast mutants devoid of yscD activity did not show any obvious alteration under a variety of different conditions, including normal growth on nonfermentable carbon sources (13). Although the mitochondrial role of *YCL57w* remains essentially uncharac-

terized, from the available data it is possible to conclude that this gene is not involved in any crucial event in mitochondrial function.

Finally, *MIP1* is functionally similar to another proteolytic component of the yeast mitochondrial import apparatus, the inner-membrane protease. This enzyme consists of two nucleus-encoded subunits, IMP1p and IMP2p, and is required for the second maturation step of imported cytochrome *b₂* and *c₁* precursors, as well as processing of the mitochondrially encoded cytochrome oxidase subunit II, and its inactivation leads to loss of respiratory competence (33, 42). Likewise, by blocking cleavage of iCoxIV and iFe-S to the corresponding mature subunits, YMIP inactivation severely affects the function of these proteins and, ultimately, the respiratory chain function. YMIP is not required for translocation of pFe-S and pCoxIV in vivo: MPP cleavage of these precursors occurs normally in *mip1* cells, and the unprocessed iFe-S and iCoxIV proteins accumulated in *mip1* mitochondria at steady state are in a trypsin-protected location. Further, the distribution of iFe-S in *mip1* mitochondria is essentially identical to that of iFe-S and mature Fe-S species in wild-type mitochondria, suggesting that YMIP is not required for sorting of the Fe-S protein to the inner membrane. On the other hand, the partitioning of unprocessed iCoxIV in *mip1* mitochondria is opposite to that of wild-type CoxIV and may reflect a sorting defect and/or the inability of iCoxIV to assemble with the other subunits of complex IV. Mistargeting of iCoxIV to the mitochondrial matrix may explain its rapid turnover in contrast with the apparent higher stability of iFe-S.

In addition to the severe defects of complexes III and IV of the respiratory chain, the biochemical consequences of *mip1* inactivation appear to include a partial defect of complex I, as indicated by 66% reduction of NADH dehydrogenase activity, and an almost complete deficiency of complex II, as indicated by a 90% reduction of succinate dehydrogenase activity. We do not know whether these results represent a primary effect of the *mip1* disruption or a secondary pleiotropic effect of the block at the level of complex III and complex IV. It is noteworthy, however, that a typical MIP-processing site is present in the targeting signal of the yeast homolog of the succinate dehydrogenase flavoprotein of complex II (36, 43), suggesting that the MIP-catalyzed maturation of this protein is also affected in *mip1* mitochondria, and we cannot exclude the possibility that one or more of the nucleus-encoded subunits of complex I also requires YMIP activity for maturation. On the other hand, because YMIP is required for maturation of only a limited number of mitochondrial precursors, its inactivation does not affect global protein import or viability, and thus YMIP should be included among the nonessential components of the yeast mitochondrial import apparatus (1).

ACKNOWLEDGMENTS

We are grateful to A. Horwich for discussions and the gift of yeast strains and plasmids, to B. Trumppower for discussions and the gift of anti-Fe-S and anticytochrome *c₁* antibodies, to G. Schatz for the gift of anti-CoxIV serum, to W. A. Fenton, F. Kalousek, and L. E. Rosenberg for discussions and critical reading of the manuscript, and to Suwon Kim for help in some experiments and discussions. We thank Genica Pharmaceuticals Corporation for performing the mitochondrial myopathies profile.

This work was supported by grant GM 48076 from National Institutes of Health. D.M. is a Howard Hughes predoctoral fellow.

REFERENCES

1. Baker, K. P., and G. Schatz. 1991. Mitochondrial proteins essential for viability mediate protein import into yeast mitochondria. *Nature (London)* **349**:205-208.

2. Beckmann, J. D., P. O. Ljungdahl, and B. L. Trumpower. 1989. Mutational analysis of the mitochondrial Rieske iron-sulfur protein of *Saccharomyces cerevisiae*. *J. Biol. Chem.* **264**:3713-3722.
3. Botstein, D., S. C. Falco, S. E. Stewart, M. Brennan, S. Scherer, D. T. Stinchcomb, K. Struhl, and R. W. Davis. 1979. Sterile host yeasts (SHY): a eukaryotic system of biological containment for recombinant DNA experiments. *Gene* **8**:17-24.
4. Bradford, M. M. 1976. A rapid and sensitive method for the quantitation of microgram quantities of protein utilizing the principle of protein-dye binding. *Anal. Biochem.* **72**:248-254.
5. Broach, J. R., J. N. Strathern, and J. B. Hicks. 1979. Transformation in yeast: development of a hybrid cloning vector and isolation of the *CAN1* gene. *Gene* **8**:121-133.
6. Cheng, M. Y., F. U. Hartl, J. Martin, R. A. Pollock, F. Kalousek, W. Neupert, E. M. Hallberg, R. I. Hallberg, and A. L. Horwich. 1989. Mitochondrial heat-shock protein hsp60 is essential for assembly of proteins imported into yeast mitochondria. *Nature (London)* **337**:620-625.
7. Cheng, M. Y., R. A. Pollock, J. P. Hendrick, and A. L. Horwich. 1987. Import and processing of human ornithine transcarbamylase precursor by mitochondria from *Saccharomyces cerevisiae*. *Proc. Natl. Acad. Sci. USA* **84**:4063-4067.
8. Daum, G., P. C. Bohni, and G. Schatz. 1982. Import of proteins into mitochondria. Cytochrome *b*₂ and cytochrome *c* peroxidase are located in the intermembrane space of yeast mitochondria. *J. Biol. Chem.* **257**:13028-13033.
9. Di Mauro, S., E. Bonilla, M. Zeviani, M. Nakagawa, and D. C. De Vivo. 1985. Mitochondrial myopathies. *Ann. Neurol.* **17**:521-538.
10. Dowhan, W., C. R. Bibus, and G. Schatz. 1985. The cytoplasmically-made subunit IV is necessary for assembly of cytochrome *c* oxidase in yeast. *EMBO J.* **4**:179-184.
11. Evan, G. I., G. K. Lewis, G. Ramsay, and J. M. Bishop. 1985. Isolation of monoclonal antibodies specific for human *c-myc* proto-oncogene product. *Mol. Cell. Biol.* **5**:3610-3616.
12. Fu, W., S. Japa, and D. S. Beattie. 1990. Import of the iron-sulfur protein of the cytochrome *bc*₁ complex into yeast mitochondria. *J. Biol. Chem.* **265**:16541-16547.
13. Garcia-Alvarez, N., U. Teichert, and D. H. Wolf. 1987. Proteinase yscD mutants of yeast. Isolation and characterization. *Eur. J. Biochem.* **163**:339-346.
14. Gavel, Y., and G. von Heijne. 1990. Cleavage-site motifs in mitochondrial targeting peptides. *Protein Eng.* **4**:33-37.
15. Graham, L. A., U. Brandt, J. S. Sargent, and B. L. Trumpower. 1993. Mutational analysis of assembly and function of the iron-sulfur protein of the cytochrome *bc*₁ complex in *Saccharomyces cerevisiae*. *J. Bioenerg. Biomembr.* **25**:245-257.
16. Hartl, F. U., N. Pfanner, D. W. Nicholson, and W. Neupert. 1989. Mitochondrial protein import. *Biochim. Biophys. Acta* **988**:1-45.
17. Hartl, F. U., B. Schmidt, E. Wachter, H. Weiss, and W. Neupert. 1986. Transport into mitochondria and intramitochondrial sorting of the Fe/S protein of ubiquinol-cytochrome *c* reductase. *Cell* **47**:939-951.
18. Hatefi, Y., and J. S. Rieske. 1967. The preparation and properties of DPNH-cytochrome *c* reductase. *Methods Enzymol.* **10**:225-231.
19. Hawlitschek, G., H. Schneider, B. Schmidt, M. Tropschug, F. U. Hartl, and W. Neupert. 1988. Mitochondrial protein import: identification of processing peptidase and of PEP, a processing enhancing protein. *Cell* **53**:785-806.
20. Hendrick, J. P., P. E. Hodges, and L. E. Rosenberg. 1989. Survey of amino-terminal proteolytic cleavage sites in mitochondrial precursor proteins: leader peptides cleaved by two matrix proteases share a three amino acid motif. *Proc. Natl. Acad. Sci. USA* **86**:4056-4060.
21. Hurt, E. C., U. Muller, and G. Schatz. 1985. The first twelve amino acids of a yeast mitochondrial outer membrane protein can direct a nuclear-encoded cytochrome oxidase subunit to the mitochondrial inner membrane. *EMBO J.* **4**:3509-3518.
22. Hurt, E. C., B. Pesold-Hurt, K. Suda, W. Oppliger, and G. Schatz. 1985. The first twelve amino acids (less than half of the presence) of an imported mitochondrial protein can direct mouse cytosolic dihydrofolate reductase into yeast mitochondrial matrix. *EMBO J.* **4**:2061-2068.
- 22a. Isaya, G. Unpublished data.
23. Isaya, G., W. A. Fenton, J. P. Hendrick, K. Furtak, F. Kalousek, and L. E. Rosenberg. 1988. Mitochondrial import and processing of mutant human ornithine transcarbamylase precursors in cultured cells. *Mol. Cell. Biol.* **8**:5150-5158.
24. Isaya, G., F. Kalousek, W. A. Fenton, and L. E. Rosenberg. 1991. Cleavage of precursors by the mitochondrial processing peptidase requires a compatible mature protein or an intermediate octapeptide. *J. Cell Biol.* **113**:65-76.
25. Isaya, G., F. Kalousek, and L. E. Rosenberg. 1992. Amino-terminal octapeptides function as recognition signals for the mitochondrial intermediate peptidase. *J. Biol. Chem.* **267**:7904-7910.
26. Isaya, G., F. Kalousek, and L. E. Rosenberg. 1992. Sequence analysis of rat mitochondrial intermediate peptidase: similarity to zinc metallopeptidases and to a putative yeast homologue. *Proc. Natl. Acad. Sci. USA* **89**:8317-8321.
27. Kalousek, F., J. P. Hendrick, and L. E. Rosenberg. 1988. Two mitochondrial matrix proteases act sequentially in the processing of mammalian matrix enzymes. *Proc. Natl. Acad. Sci. USA* **85**:7536-7540.
28. Kalousek, F., G. Isaya, and L. E. Rosenberg. 1992. Rat liver mitochondrial intermediate peptidase (MIP): purification and initial characterization. *EMBO J.* **11**:2803-2809.
29. Kawabata, S., K. Nakagawa, T. Muta, S. Iwanaga, and E. W. Davie. 1993. Rabbit liver microsomal endopeptidase with substrate specificity for processing proproteins is structurally related to rat testes metalloendopeptidase 24.15. *J. Biol. Chem.* **268**:12498-12503.
30. King, T. E., and R. L. Howard. 1967. Preparations and properties of soluble NADH dehydrogenase from cardiac muscle. *Methods Enzymol.* **10**:275-294.
31. Kleiber, J., F. Kalousek, M. Swaroop, and L. E. Rosenberg. 1990. The general mitochondrial matrix processing protease from rat liver: structural characterization of the catalytic subunit. *Proc. Natl. Acad. Sci. USA* **87**:7978-7982.
32. Loewenstein, J., H. R. Scholte, and E. M. Wit-Peeters. 1970. A rapid and simple procedure to deplete rat liver mitochondria of lysosomal activity. *Biochim. Biophys. Acta* **223**:432-436.
33. Nunnari, J., T. D. Fox, and P. Walter. 1993. A mitochondrial protease with two catalytic subunits of nonoverlapping specificities. *Science* **262**:1997-2004.
34. Oliver, S. G., et al. 1992. The complete DNA sequence of yeast chromosome III. *Nature (London)* **357**:38-46.
35. Pollock, R. A., F.-U. Hartl, M. Y. Cheng, J. Ostermann, A. L. Horwich, and W. Neupert. 1988. The processing peptidase of yeast mitochondria: the two cooperating components MPP and PEP are structurally related. *EMBO J.* **7**:3493-3500.
36. Robinson, K. M., and B. D. Lemire. 1992. Isolation and nucleotide sequence of the *Saccharomyces cerevisiae* gene for the succinate dehydrogenase flavoprotein subunit. *J. Biol. Chem.* **267**:10101-10107.
37. Rose, M. D., P. Novick, T. H. Thomas, D. Botstein, and G. R. Fink. 1987. A *Saccharomyces cerevisiae* genomic plasmid bank based on a centromere-containing shuttle vector. *Gene* **60**:237-243.
38. Rose, M. D., F. Winston, and P. Hieter. 1990. *Methods in yeast genetics: a laboratory manual*. Cold Spring Harbor Laboratory Press, Cold Spring Harbor, N.Y.
39. Rothstein, R. 1991. Targeting, disruption, replacement, and allele rescue: integrative DNA transformation in yeast. *Methods Enzymol.* **194**:281-301.
40. Sambrook, J., E. F. Fritsch, and T. Maniatis. 1989. *Molecular cloning: a laboratory manual*, 2nd ed. Cold Spring Harbor Laboratory, Cold Spring Harbor, N.Y.
41. Schnaitman, C., and J. W. Greenawalt. 1968. Enzymatic properties of the inner and outer membranes of rat liver mitochondria. *J. Cell Biol.* **38**:158-175.
42. Schneider, A., M. Behrens, P. Scherer, E. Pratz, G. Michaelis, and G. Schatz. 1991. Inner membrane protease I, an enzyme mediating intramitochondrial protein sorting in yeast. *EMBO J.* **10**:247-254.
43. Schulke, N., G. Blobel, and D. Pain. 1992. Primary structure, import and assembly of the yeast homologue of succinate dehy-

- drogenase flavoprotein. Proc. Natl. Acad. Sci. USA **89**:8011–8015.
44. **Sherman, F.** 1967. The preparation of cytochrome-deficient mutants of yeast. *Methods Enzymol.* **10**:610–616.
45. **Sherman, F.** 1991. Getting started with yeast. *Methods Enzymol.* **194**:3–21.
46. **Sikorski, R. S., and P. Hieter.** 1989. A system of shuttle vectors and yeast host strains designed for efficient manipulation of DNA in *Saccharomyces cerevisiae*. *Genetics* **122**:19–27.
47. **Srere, P. A.** 1969. Citrate synthase. *Methods Enzymol.* **13**:3–11.
48. **Stitt, M.** 1983. Fumarase, p. 359–362. *In* H. U. Bergmeyer (ed.), *Methods of enzymatic analysis*, 3rd ed., vol. 4. Verlag Chemie, Weinheim, Germany.
49. **Tisdale, H. D.** 1967. Preparation and properties of succinic-cytochrome *c* reductase. *Methods Enzymol.* **10**:213–215.
50. **Tislar, U.** 1993. Thimet-oligopeptidase—a review of a thiol dependent metallo-endopeptidase also known as Pz peptidase, endopeptidase 24.15, and endo-oligopeptidase. *Biol. Chem. Hoppe-Seyler* **374**:91–100.
51. **Tropshug, M., D. W. Nicholson, F. U. Hartl, H. Kohler, N. Pfanner, E. Wachter, and W. Neupert.** 1988. Cyclosporin A-binding protein (cyclophilin) of *Neurospora crassa*. One gene codes for both the cytosolic and mitochondrial forms. *J. Biol. Chem.* **263**:14433–14440.
52. **van Loon, A. P. G. M., A. W. Brandli, and G. Schatz.** 1986. The presequences of two imported mitochondrial proteins contain information for intracellular and intramitochondrial sorting. *Cell* **44**:801–812.
53. **Vassarotti, A., W. J. Chen, C. Smagula, and M. G. Douglas.** 1987. Sequences distal to the mitochondrial targeting sequences are necessary for the maturation of the F₁-ATPase β -subunit precursor in mitochondria. *J. Biol. Chem.* **262**:411–418.
54. **West, A. H., D. J. Clark, J. Martin, W. Neupert, F.-U. Hartl, and A. L. Horwich.** 1992. Two related genes encoding extremely hydrophobic proteins suppress a lethal mutation in the yeast mitochondrial processing enhancing protein. *J. Biol. Chem.* **267**:24625–24633.
55. **Wharton, D. C., and A. Tzagoloff.** 1967. Cytochrome oxidase from beef heart mitochondria. *Methods Enzymol.* **10**:245–250.
56. **Yaffe, M. P.** 1991. Analysis of mitochondrial function and assembly. *Methods Enzymol.* **194**:627–643.
57. **Yang, M., R. E. Jensen, M. P. Yaffe, W. Opplinger, and G. Schatz.** 1988. Import of proteins into yeast mitochondria: the purified matrix processing protease contains two subunits which are encoded by nuclear MAS1 and MAS2 genes. *EMBO J.* **7**:3857–3862.
58. **Ziegler, D., and J. S. Rieseke.** 1967. Preparation and properties of succinate dehydrogenase-coenzyme Q reductase. *Methods Enzymol.* **10**:231–235.